

# COMPLEXITIES IN THE ESTIMATION OF EMISSIONS AND IMPACTS OF WIND GENERATED FUGITIVE DUST

Lucian W Burger

AIRSHED PLANNING PROFESSIONALS (PTY) LTD, 30 Smuts Rd, Midrand, Gauteng, 1685, South Africa, [lucian@airshed.co.za](mailto:lucian@airshed.co.za)

## Abstract

Wind-generated emissions from open dust sources exhibit a high degree of variability from one site to another, and emissions at any one site tend to fluctuate widely. The site characteristics which cause these variations may be grouped into

- properties of the exposed surface material from which the dust originates, and
- measures of energy expended by wind interacting with the erodible surface.

Many theoretical emission rate models have been developed to accommodate these characteristics and range from relatively simple analytical and semi-analytical ones to more complicated numerical models. Dust emissions are the vertical mass flux of dust at the surface. Typically, the more simplistic models provide a single expression for the vertical mass flux, whereas the more complicated models attempt to derive the vertical flux from the horizontal mass flux. The horizontal flux is calculated using knowledge of the dry-particle size distribution of the exposed soil or surface material, and most importantly particles ranging in diameter from about 75 to 500  $\mu\text{m}$  that are readily lifted from the surface and jump or bounce within a layer close to the air-surface interface. This is also known as saltation. Saltation provides energy for the release of fine particles that typically are bound by surface forces to larger clusters.

These emission models can provide very different emission rates depending on the input data, assumptions of the surface material and the specific model approach. These differences are further enhanced when applications of the model ignore real-life factors such as the occurrence of nonerodible elements, crust formation and actual wind behaviour (e.g. short duration gusts).

The paper provides a comparison of different wind-generated dust emission rate models, the potential error when used to determine air quality impacts and recommendations.

*Keywords:* wind erosion, dust emission rate models, dust model comparison.

## 1. Introduction

Few realise that the beauty of a romantic African sunset is a result of scattering of sunlight by airborne particles. This beauty may be admirable from a distance, but closer to the source, dust particles can be the cause of significant soiling, damage to property, loss of production and adverse health impacts.

Dust generated through wind erosion is a significant contributor to this sunset. Estimations of global dust emissions range from 500 million t/yr (Peterson and Junge, 1971) to 3000 million t/yr (Tegen and Fung, 1994). Recent estimates are

converging to a value between 1000 million t/yr to 2000 million t/yr (Zender *et al*, 2003; Ginoux *et al*, 2004, Miller *et al*, 2004; Tanaka and Chiba, 2006). About 80% of this dust is from the Northern Hemisphere, which is not surprising, given that the world's largest source of dust is the Sahara Desert. The estimated range of dust emission from the Sahara Desert is from 130 million t/yr (Swap *et al*, 1996) to 760 million t/yr (Callot *et al*, 2000).

Tegen and Fung (1995) carried out an analysis of potential areas of wind erosion over the world and showed that about 30% to 50% of the total dust emissions can be attributed to disturbed soil surfaces and the rest to natural soil surfaces. In

Africa approximately 54% is from desert and sparsely vegetated soils.

### 1.1. Mechanism of wind erosion

The modelling work of Tegen and Fung (1994) indicates that the global dust emissions consists of 13% in the particle size group of 0.5 to 1  $\mu\text{m}$ , 65% in the group of 1 to 35  $\mu\text{m}$ , and 22% in the group of 35 to 50  $\mu\text{m}$ . Dust entrained into the atmosphere originates in soils which contain clay-sized (particle diameters of less than 2.5  $\mu\text{m}$ ) and silt sized (between 2.5  $\mu\text{m}$  and 60  $\mu\text{m}$ ) particles. However, the clay and silt-sized particles are not directly mobilised by the wind because cohesive forces (e.g. capillary and electrostatic) bind these particles tightly to the soil. Dust is primarily injected into the atmosphere during sandblasting caused by saltation bombardment (Figure 1) (Alfaro and Gomes, 2001; Grini *et al.*, 2002). Saltation of sand-sized particles (particles larger than 60  $\mu\text{m}$ ) is the horizontal movement of soil grains in a turbulent near surface layer. The bulk of total transport (50 to 80%) is by saltation. Most saltation particles rise less than 1.2 m, with the majority less than 300 mm.

A third mode of motion is known as surface creep and applies to relatively large soil particles (typically larger than 0.5 mm). Surface creep constitutes 7 to 25 % of total transport. Typically only 1% by mass, but mostly less than 10 %, are carried to high altitudes and suspended over long distances.

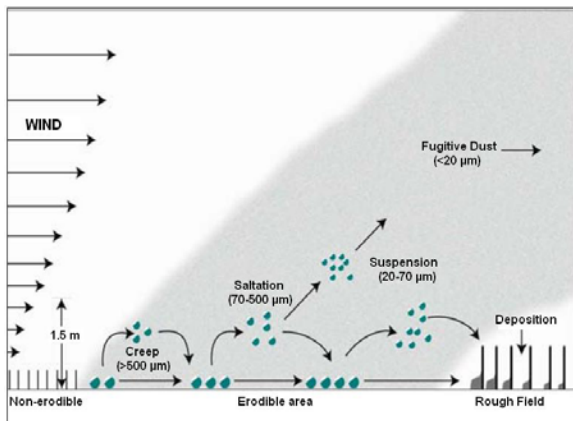


**Figure 1: Illustration of creep, saltation and suspension of soil particulates during an erosion event**

### 1.2. Factors influencing wind erosion

The various factors that influence the rate of wind erosion are given below:

- **Soil texture.** Loamy sand, rich in particles between 10 and 100  $\mu\text{m}$  in size, is the most vulnerable soil (Bagnold 1937). More clayey soil is much stickier, better-structured, and hence more resistant. Coarse sand and

gravelly or rocky soils are also more resistant, since the particles are too heavy to be removed by wind erosion.

- **Soil structure.** The less structure-improving matter a soil has on the surface (organic matter, iron and free aluminium, lime), the more fragile it will be, while the presence of sodium or salt often leads to formation of a layer of dust on the surface, which fosters wind erosion.
- **State of the soil surface.** If the soil surface is stony, forming a "pavement", the risks of wind erosion are lower. A rough surface, left by cloddy tillage or ridges perpendicular to the prevailing wind, slows down the wind at ground level, thus reducing saltation.
- **Vegetation.** Stubble and crop residues in the soil cut wind-speed at ground level.
- **Soil moisture.** Moisture increases cohesion of sand and loam, temporarily preventing their erosion by wind.
- **Frequency of disturbance.** Frequently disturbed surfaces cause break-up of crusty soils and/or mixing of material beneath leaving a refreshed reservoir for wind erosion.

### 1.3. Mechanism of dust mass flux

Shao (2008) proposes three dust-emission mechanisms to describe the vertical mass flux, as depicted in Figure 2. With aerodynamic lift, dust particles can be lifted from the surface directly by aerodynamic forces, however as the importance of gravity and aerodynamic forces diminishes for smaller particles and inter-cohesion becomes more important, dust emission arising from this mechanism is small in general.

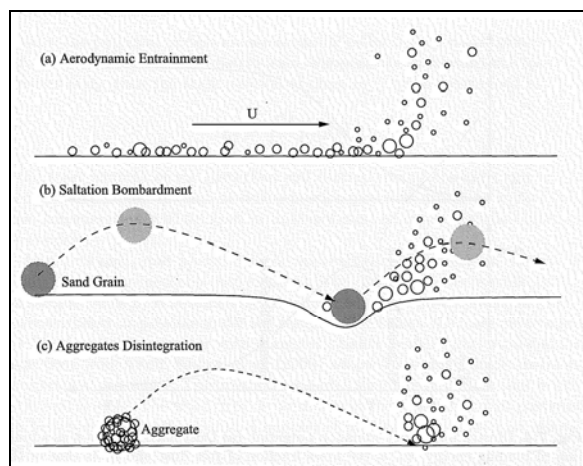


**Figure 2: Mechanism for dust emission. (a) By aerodynamic lift, (b) saltation bombardment, (c) disaggregation (reproduced from Shao 2008)**

With saltation bombardment, particles strike the surface and cause localised impacts which are

strong enough to overcome the binding forces acting upon dust particles leading to dust emissions. This mechanism can be an order of magnitude larger than the aerodynamic entrainment.

Disaggregation occurs when particles are released from aggregates in soil typically with high clay content. During a weak wind erosion event, sand particles coated with dusts behave as individuals and dust particles may not be released. During strong wind-erosion events, dustcoats and aggregates may disintegrate resulting in increased dust emissions.

## 2. Dust emissions models

### 2.1. Vertical mass flux

Dust is mobilised from dry soil surfaces when the wind exceeds specific wind speeds, typically about 6 m/s, but varies according to soil and surface characteristics. Most wind erosion models, however, use friction velocity ( $u_*$ ) instead of the wind speed to calculate the rate of dust generation. The friction velocity represents a measure of wind shear stress on the erodible surface, as is determined from the slope of the wind speed profile. Since the friction velocity reflects the wind conditions closest to the surface, its use is preferred over the use of the wind speed. The mass flux of particles depends on the excess of the wind friction speed  $u_*$  over the threshold wind friction speed for saltation,  $u_{*t}$ .

Since the friction velocity is a measure of available energy, the most basic formulations for vertical flux  $F$  ( $\text{g}/\text{cm}^2\text{-s}$ ) have been developed to fit the form:

$$F = \alpha u_*^n$$

with  $u_*$  in m/s,  $n$  ranging between 2.9 and 4.4 (Gillette 1977) and  $\alpha$  an empirical constant, which typically varies from  $10^{-7}$  to  $10^{-5}$   $\text{g}/\text{m}^{n+2}\text{s}^{1-n}$ . The parameters  $\alpha$  and  $n$  depend strongly on the soil type.

Based on experimental evidence, Shao (2008) proceeded to illustrate that these hypotheses are restrictive in their use and that they do not support experimental evidence, especially at low threshold friction velocities where over-predictions could be by a few orders of magnitude. Other variations of the above relationship include:

$$F = \alpha_g u_*^4 (1 - u_{*t}/u_*)$$

with  $\alpha_g$  an experimentally derived constant (Gillette and Passi 1985) and

$$F = \alpha_1 (u_* - u_{*t})^2 + \alpha_2 (u_* - u_{*t})$$

with  $\alpha_1=1.6 \times 10^{-6}$  and  $\alpha_2=6.9 \times 10^{-7}$  (Cowherd *et al* 1988)<sup>1</sup>.

As discussed in the previous section, vertical flux can be described by three mechanisms, namely aerodynamic lift, saltation bombardment and aggregate disintegration. Loosmore and Hunt (2000) carried out wind-tunnel experiments on uncrusted fine material and found that the vertical flux due to aerodynamic lift was significantly lower than saltation bombardment (few orders of magnitude). It is therefore not unreasonable to relate the vertical dust flux to the saltation, or horizontal flux. In fact, whereas the horizontal flux  $Q$  (see next section) is linearly related to  $u_*^3$ ,  $F/Q$  is almost independent of  $u_*$  suggesting that  $F$  can be determined from  $Q$ . The horizontal mass flux is converted to the vertical dust mass flux with an efficiency  $\eta$ , called the sandblasting mass efficiency (Alfaro *et al.*, 1997), i.e.,  $F = \eta Q$ . Observations reveal that  $\eta$  exhibits high sensitivity to parent soil texture.

Marticorena and Bergametti (1985) developed a relatively simplistic empirical relationship relating clay percentage  $M_{\text{clay}}$  to  $\eta$  as follows:

$$\eta = 10^{[0.134M_{\text{clay}} - 6]}$$

where  $M_{\text{clay}}$  is the the clay percentage of the surface material. In this formulation, the sandblasting effect was not explicitly dealt with.

Saltation-sandblasting produces dynamic dust size distributions which changes with wind friction velocity (Iversen and White, 1982). The dust aerosol size released by sandblasting depends on saltator kinetic energy. Thus the dust size distribution depends on the parent soil aggregate size distribution and the wind friction velocity. High kinetic energy saltators release small dust aerosols and low kinetic energy saltators release large dust aerosols (Shao *et al*, 1993). The difficulty in development an equivalent model for  $\eta$ , taking into account the sandblasting effect with currently available knowledge is illustrated by Shao (2008). Shao nonetheless provides an approximate relationship using particle size dependence:

$$\beta = 10^{-5} [1.25 \ln(d_s) + 3.28] \exp(-140.7 d_d + 0.37)$$

where  $d_s$  and  $d_d$  are the saltator and dust particle sizes, respectively in mm. The vertical dust flux is then expressed as:

<sup>1</sup> The equation has been adopted from the original form in order to compare the emission units for  $F$  of  $\text{g}/\text{cm}^2\text{-s}$ .

$$F = \beta Q u_*^{-2}$$

In more complex numerical treatments, the models attempt to treat the emission of individual particles based on their respective energy balances.

## 2.2. Horizontal mass flux

As discussed in Section 1.1, saltation is the most important mode of horizontal flux and the driving forces for vertical flux. A range of saltation models has been developed from simple analytical and semi-empirical formulations for idealised situations to more complicated formulations which have to be solved numerically. Table 1 is a summary of the most referenced analytical models used to describe horizontal flux. Clearly, the horizontal flux exhibits a  $u_*^3$ -dependence in all of these forms. Other than scaling effects (i.e. the  $c_0$  constant), the only difference between the different formulations appears to be due to the refinement around the threshold friction velocity, i.e. reducing the flux when the friction velocity approaches the threshold friction velocity.

**Table 1: Summary of different saltation models**

	Expression	Constant
(a)	$Q = c_0 \left( \frac{d}{D} \right)^{1/2} \frac{\rho}{g} u_*^3$	D=250 $\mu\text{m}$
		$C_0=1.5$ [uniform sand]
		$C_0=1.8$ [natural sand]
		$C_0=2.8$ [poorly sorted sand]
(b)	$Q = c_0 \left( \frac{d}{D} \right)^{3/4} \frac{\rho}{g} u_*^3$	D=250 $\mu\text{m}$ $C_0=0.83$
(c)	$Q = c_0 \frac{\rho}{g} u_*^3 (1-R)(1+R)^2$	$C_0=1.8$ to $3.1$
(d)	$Q = c_0 \frac{\rho}{g} u_*^3 (1-R)(1+R)^2$	$C_0=2.6$
(e)	$Q = c_0 \frac{\rho}{g} u_*^3 (1-R^2)$	$C_0=0.25 + \frac{w_t}{3u_*}$
(f)	$Q = c_0 \left( \frac{d}{D} \right)^{1/2} \frac{\rho}{g} u_*^3 (1-R)$	D=250 $\mu\text{m}$ $C_0=4.2$

Notes: (a) Bagnold (1937); (b) Zingg (1953); (c) Kawamura (1964); (d) White (1979); (e) Owen (1964); and (f) Lettau and Lettau (1978). With  $R = u_{*t}/u_*$  and  $w_t$  the particle terminal velocity.

## 2. Flux model performances

Figure 3 summarises the horizontal flux model performances as given in Table 1. A fairly significant difference in the results is observed,

ranging from a factor of 3 to 10 from each other. The differences are relatively constant at higher friction velocities, clearly reflecting the different scaling values. At friction velocities closer to the threshold friction velocity (i.e. 0.2 m/s in this example), significant deviations occur between the curves. As expected, the Bagnold (1937) and Zingg (1953) formulations do not have a gradual reduction, as shown by the others. Shao (2008) pointed out that the difference in scaling is perhaps more a reflection of the nature of saltation which contains a large degree of randomness that cannot be described precisely by these simple forms. Nevertheless, Shao recommends using the equations by Kawamura (1964), Owen (1964) and Lettau & Lettau (1978).

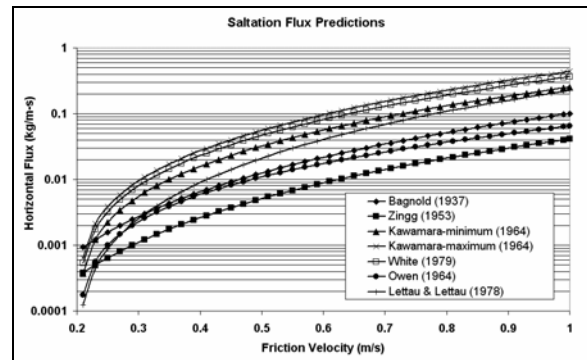


**Figure 3: Comparison of saltation flux predictions for particles with a diameter of 75  $\mu\text{m}$**

Figure 4 is a comparison of vertical flux models, including the relatively simple forms of Gillette (1977), Gillette and Passi (1985) and Cowherd *et al* (1988). The Marticorena and Bergametti (1985) and Shao (2008) equations used the Kawamura (1964) form of the horizontal flux with the coefficient proposed by White (1979). In this example, 5% clay content was used in the Marticorena and Bergametti (1985) mode. A lognormal particle size distribution was assumed for saltator sizes in the Shao (2008) model.

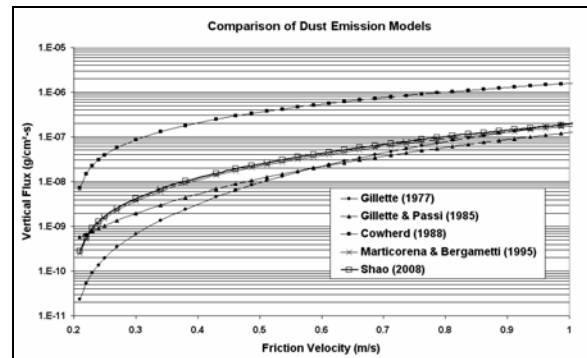


**Figure 4: Comparison of vertical flux model predictions**

Apart from the Cowherd *et al* (1988) model, there appears to be a relatively good grouping between the others, particularly at higher friction velocities. At friction velocities closer to the threshold friction velocity significant deviations exist between the simplistic approaches (Gillette (1977) and Gillette and Passi (1985)) and the forms based on a scaling of the horizontal flux. Although the methods of Marticorena and Bergametti (1985) and Shao (2008) provide similar results in this example, the former is based on an empirical approach whereas the latter is based on a theoretical treatment of the particle behaviours.

### 3 Friction velocity

The friction velocity is a measure of the available momentum flux from the atmosphere to the surface. In routine calculations, this parameter is derived from wind speed measurements at a fixed height, typically 10m. Most applications use a logarithmic wind profile, although this form is only applicable under neutral atmospheric conditions:

$$u(z) = \frac{u_*}{\kappa} \ln\left(\frac{z}{z_0}\right)$$

where  $\kappa$  is the von Karman constant (~0.4) and  $z_0$  the aerodynamic roughness length. However, this profile can potentially be significantly modified under stable and unstable atmospheric conditions. The unstable wind profile approaches “plug flow” and hence a higher  $u_*$  for the same wind speed, whereas a stable wind profile results in a smaller  $u_*$  for the same wind speed. Since the horizontal flux is strongly dependent on  $u_*$  (i.e. to a power of ~3), using the correct  $u_*$  is very important in estimating the wind erosion.

### 4 Threshold friction velocity

The mechanisms for dust emission involve the saltation of sand-sized particles and the transfer of momentum from the atmosphere to the surface. The eventual movement of soil surface particles is due to adequate driving forces available to overcome retarding forces. The driving forces include aerodynamic drag and aerodynamic lift, whilst the retarding forces include gravity and inter-particle cohesive forces.

The threshold friction velocity ( $u_{*t}$ ) is the minimum friction velocity required for the driving forces to overcome the retarding forces to initialise the movement of soil particles. The  $u_{*t}$  therefore describes the capacity of the surface to resist wind erosion and is affected by a range of factors as discussed previously in Section 1.2, and below.

#### 4.1. Soil particle size

Under ideal conditions,  $u_{*t}$  can be expressed as a function of only particle size,  $u_{*t}(d)$ . The optimal particle size for saltation occurs where  $u_{*t}$  is at a minimum. Figure 5 show that for typical soil conditions, the highest saltation occurs with particle sizes of about 75  $\mu\text{m}$  (Iversen and White, 1982). For particles smaller than 75  $\mu\text{m}$ ,  $u_{*t}$  increases due to the effect of adhesive forces. For larger particles, gravitational forces hold the particles in bed.

#### 4.2. Momentum partitioning

Several theories for  $u_{*t}$  have been derived for soils with uniform and spherical particles spread loosely over dry and unsheltered surfaces. In reality, the soil surface is made up of varying particles sizes and roughness elements. These subsequently influence the transfer of momentum through the partition of total momentum flux into a pressure drag on roughness elements and a skin drag on substrate surface. Surface roughness therefore aids to ameliorate wind erosion by extracting a portion of the wind's momentum thereby reducing the quantity of stress on the surface. The resulting  $u_{*t}$  therefore increases with increasing roughness. Marticorena and Bergametti (1985) developed a relatively simplistic correction factor to adjust  $u_*$  to account for non-uniform particle size conditions, also known as the *wind friction efficiency*. This generally leads to increased values for  $u_{*t}$ , resulting in near zero flux when a large fraction of particles of 10 mm and larger are present. Gross over-predictions can therefore occur if this correction is not applied.

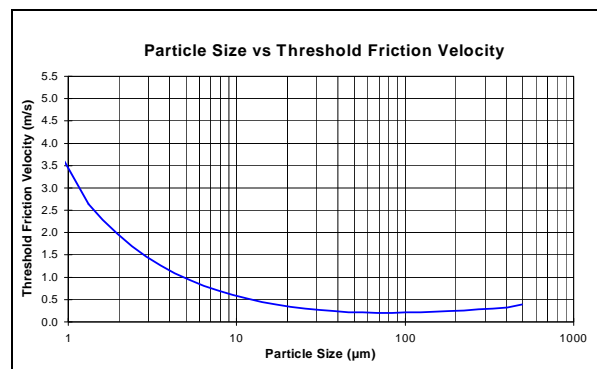


Figure 5: Relationship between particle sizes and threshold friction velocities (Iversen and White, 1982)

#### 4.3. Drag partitioning

Owen (1964) showed that the saltation layer which develops during wind erosion events acts as an additional sink of atmospheric momentum, causing an increase in momentum deposition to the surface and thus an increase in roughness length. Saltating particles mediate this effect by removing

momentum from the atmosphere and transferring it to the surface during each (non-ballistic) impact. This is also known as the *Owen effect*. Gillette *et al* (1998) found that the increase in wind friction speed due to saltation varies quadratically with the difference between the 10m wind speed  $u_{10}$  and the threshold wind speed at 10m  $u_{10t}$  as

$$\Delta u_* = 0.003(u_{10} - u_{10t})^2$$

with all speeds in m/s. Neglecting the Owen effect would therefore cause significant under-prediction of saltation.

#### 4.4. Soil moisture

Soil moisture increases the erosion threshold due to reinforcement of soil cohesion. Soil water retention consists of (a) molecular adsorption on the soil grain surface and (b) capillary forces between the grains. The inter-particle forces due to the adsorption film are much lower than the inter-particle capillary forces, and therefore the latter forces are the main factor responsible for the increase of the wind erosion threshold observed when the soil moisture increases.

So, when the soil moisture content is close to but smaller than the maximum amount of adsorbed water, these capillary forces are considered as not strong enough to significantly increase the erosion threshold.

The absorbed water ( $w'$ ) can be calculated using the relationship developed by Fecan, Marticorena and Bergametti (1999) and is given as

$$w' = 0.0014M_{clay}^2 + 0.17M_{clay}$$

For a high clay content of 50%, as in your example, the mass water content  $w' = 12\%$ . Therefore, if the total soil moisture is below this value, the capillary water induces negligible cohesion forces. The clayey component of the soil is known to influence the adsorption capacity of the soil, since it is responsible for electrostatic forces that maintain the water at the grain surface. This suggests that  $w'$  is related to the maximum amount of water that can be retained in the soil by the adsorption films forming at the surface of the soil grains. The limitations of this parameterization are linked to the main hypothesis on which it is based, i.e. that the capillary forces are responsible for threshold increases observed when the soil moisture increases and the adsorption processes do not induce significant inter-particle cohesion forces and due to the lack of a precise description of the water separation in the soil matrix.

#### 4.5. Surface crust

Following the wetting of a soil or other surface material, fine particles will move to form a surface crust. The surface crust acts to hold in soil moisture

and resist erosion. The degree of protection that is afforded by a soil crust to the underlying soil may be measured by the modulus of rupture (roughly a measure of the hardness of the crust) and thickness of the crust.

Goossens (2004) measured the physical crust strength at 45 locations in Germany and developed relationships between crust strength ( $\tau$ ) and the horizontal ( $Q$ ) and vertical ( $F$ ) fluxes. The ratio of the uncrusted ( $Q$ ) to the crusted ( $Q_c$ ) horizontal flux was shown to fit the following expression:

$$\frac{Q}{Q_c} = 5.2\left(\frac{\tau}{10}\right)^6 - 55\left(\frac{\tau}{10}\right)^5 + 201.6\left(\frac{\tau}{10}\right)^4 - 300.6\left(\frac{\tau}{10}\right)^3 + 255.2\left(\frac{\tau}{10}\right)^2 - 15.8\left(\frac{\tau}{10}\right) + 1$$

with ( $\tau$ ) in kPa. Both fluxes decreased exponentially as the surface crust became stronger. The study also suggests that the gradual bombardment of a surface crust by impacting particles does not immediately result in a decay of the crust's protective effect, provided that the crust has a minimum thickness. However, once the crust becomes perforated, its protective effect disappears very quickly, leading to much higher horizontal and vertical sediment fluxes than predicted for undamaged crusted soil.

#### 4.6. Averaging time

Many theoretical equations have been developed for  $u_{*t}$  based on various averaging periods, ranging from a few minutes to hourly averages. Routine calculations are normally based on hourly average wind speed. The question then arises whether or not the averaging time of wind speed measurement affects the observed wind speed threshold.

Stout (1998) used wind speed data taken at 1 Hz and simultaneously measuring saltation activity with a piezoelectric saltation sensor. It was possible to calculate  $u_{*t}$  using the same data set averaged over periods of 2, 5, 10, 20, 30, and 60 seconds. The results reveal that, under typical field conditions with gusty turbulent winds, long averaging times produce an apparent threshold that is considerably lower than the true wind speed at which saltation is initiated. Based on these findings it is possible to show that the under-prediction would be less than 20%.

## 5 Conclusions

The two most important fundamental parameters that influence the accuracy of calculating dust emissions are the friction velocity and the threshold friction velocity. The former provides the amount of

wind energy available to generated dust, whereas the latter is a measure of resistance against the wind strength. Dust emissions are very sensitive to the  $u_*$  (to the power  $\sim 3$ ), but only if it exceeds  $u_{*t}$ . A relatively small 10% error in the  $u_*$  can cause more than a 2-fold error when  $u_*$  is near  $u_{*t}$ . This error decreases to about 30% at much higher friction velocities (i.e.  $>2u_{*t}$ ). Similarly, under- or over-predicting  $u_{*t}$ , can result in significant over- or under prediction, respectively at low wind speeds. A well-defined, repeatable methodology could ensure consistency in the results. It is therefore best to avoid subjective specification of parameters such as the aerodynamic roughness lengths ( $z_0$ ). These should preferably be determined from measurable input parameters, such as a comprehensive particle size distribution set. It is also important to use the correct wind profile, which is applicable to the prevailing atmospheric stability.

The quantification  $u_{*t}$  must take into account all factors that could be of influence, e.g. soil particle size, moisture content, surface covering and surface crusting tendency. Ignoring any of these could result in significantly wrong answers.

It was also shown that the use of wind data averaged over relatively long periods could potentially result in under-predictions of dust emissions. However, this error reaches a maximum under-prediction of only about 20%.

Although the use of different flux models can produce widely different results (order of magnitude), it was illustrated that some of the more recent analytical models converge on producing similar results to each other. It is therefore recommended to use vertical flux models that are based on quantifying the horizontal flux, such as the Marticorena and Bergametti (1985) and Shao (2008) models. The most appropriate selection of a horizontal flux model is not as obvious. However, following the notion of Shao (2008), the models developed by Kawamura (1964), Owen (1964) and Lettau & Lettau (1978) are recommended.

## References

Alfaro, S. C. and L. Gomes, 2001: Modeling mineral aerosol production by wind erosion: Emission intensities and aerosol size distributions in source areas. *J. Geophys. Res.*, **106**(D16), 18075–18084.

Alfaro, S. C., A. Gaudichet, L. Gomes, and Maille M (1997), Modeling the size distribution of a soil aerosol produced by sandblasting, *J. Geophys. Res.*, **102**, 11,239–11,249

Bagnold, R. A (1937) The Transport of sand by wind, *Geogr J*, **89**, 409-438

Callot Y, B Marticorena. and G. Bergametti (2000) Geomorphologic approach for modelling the surface features of arid environments in a model of dust emissions: application to the Sahara desert, *Geodinamica Acta*, **13**, 245-270

Cowherd C, Muleski GE and Kinsey J S (1988), *Control Of Open Fugitive Dust Sources*, EPA 450/3-88-008, U. S. Environmental Protection Agency, Research Triangle Park, NC

Fecan, F., B. Marticorena and G. Bergametti, (1999): Parametrization of the increase of the Aeolian erosion threshold wind friction velocity due to soil moisture for arid and semi-arid areas. *Annales Geophysicae*, **17**, 149–157.

Gillette, D. A. (1977) Fine particle emissions due to wind erosion, *Trans Am Soc Agric Engrs*, **20**, 890-987

Gillette, D. A., B. Marticorena and G. Bergametti, (1998) Change in the aerodynamic roughness height by saltating grains: Experimental assessment, test of theory, and operational parameterization. *J. Geophys. Res.*, **103**(D6), 6203–6209.

Gillette, D. A. and R. Passi (1988) Modeling dust emission caused by wind erosion. *J. Geophys. Res.*, **93**(D11), 14233–14242

Ginoux, P, J M Prospero, O Torres and MChin (2004). Long-term simulation of global dust distribution with the GOCART model: correlation with North Atlantic Oscillation. *Env Modelling & Software*, **19**, 113-128

Goossens D (2004) Effect of soil crusting on the emission and transport of wind-eroded sediment: field measurements on loamy sandy soil, *Geomorphology*, **58**, 145–160

Grini, A., C. S. Zender and P. Colarco, (2002) Saltation sandblasting behavior during mineral dust aerosol production. *Geophys. Res. Lett.*, **29**(18), 1868

Iversen, J. D. and B. R. White (1982) Saltation threshold on Earth, Mars, and Venus. *Sedimentology*, **29**, 111–119.

Kawamura R (1964) Study of sand movement by wind. In: Hydraulic Eng. Lab. Tech Rep. University of California, Berkely, CA, HEL-2-8, pp 99-108

Lettau K and H H Lettau (1978) Experimental and micrometeorological field studies of dune migration. In: Lettau HH and K Lettau (ds) Exploring the World's Driest Climate, University of Wisconsin, Madison, WI, pp 110-147

Loosemore G A and JR Hunt (2000) Below-threshold, non-abraded dust resuspension. *J. Geophys Res*, **105**(20), 663-20, 671

Marticorena, B. and G. Bergametti (1995) Modeling the atmospheric dust cycle: 1. Design of a soil-

- derived dust emission scheme. *J. Geophys. Res.*, **100**(D8), 16415–16430.
- Miller R, I Tegen, Z Perlwitz (2004) Surface radiative forcing by soil dust aerosols and the hydrologic cycle, *J. Geophys. Res.*, **109**(D4), D04, 203, doi:10.1029/2003JD004,085.
- Owen, P. R. (1964) Saltation of uniform grains in air. *J. Fluid. Mech.*, **20**(2), 225–242.
- Peterson S T and CE Junge (1971) Sources of particulate matter in the atmosphere. In: Kellogg WW and GD Robinson (eds) *Man's Impact on the Climate*, MIT Press, pp 310-320
- Shao Y (2008) *Physics and Modelling of wind erosion, Atmospheric and Oceanographic Science library, 2<sup>nd</sup> Revised and Expanded Edition*, Springer
- Shao, Y., M. R. Raupach and P. A. Findlater, 1993: Effect of saltation bombardment on the entrainment of dust by wind. *J. Geophys. Res.*, **98**(D7), 12719–12726.
- Stout JE (1998) Effect of averaging time on the apparent threshold for aeolian transport, *Journal of Arid Environments*, **39**: 395–401
- Swap R, S Ulanski, M Cobette, M Garsgang (1996) Temporal and spatial characteristics of sharan dust outbreaks. *J. Geophys. Res.*, **101**(D2), 4205-4220
- Tanaka T Y and M Chiba (2006) A numerical study of the contributions of dust source regions to the global dust budget. *Global Planet Change*, **52**, 88-104
- Tegen I and I Fung (1994) Modeling of mineral dust in the atmosphere: sources, transport, and optical thickness. *J. Geophys. Res.*, **99**, 22897-22914
- Tegen I and I Fung (1995) Contribution to the atmospheric mineral aerosol load from land surface modification. *J. Geophys. Res.*, **100**, 18707-18726
- White, B. R. (1979) Soil transport by winds on Mars. *J. Geophys. Res.*, **84**(B9), 4643–4651
- Zender, C. S., H. Bian and D. Newman, 2003a: Mineral Dust Entrainment And Deposition (DEAD) model: Description and 1990s dust climatology. *J. Geophys. Res.*, **108**(D14), 4416
- Zingg A W (1953) Wind-tunnel studies of the movement of sedimentary material. In: *Proceedings of the 5<sup>th</sup> Hydraulic Conference*, University of Iowa Studies in Engineering, Iowa City, IA, 34, pp111-135